Journal of Alloys and Compounds 508 (2010) 24–27

Contents lists available at ScienceDirect

Journal of Alloys and Compounds

journal homepage: www.elsevier.com/locate/jallcom

Crystallographic and spectroscopic characterization of $LnFeTeO_6$ (Ln = La, Pr, Nd, Sm) materials

Araceli E. Lavat[a], Roberto C. Mercader[b], Enrique J. Baran[c,*]

[a] Departamento de Ingeniería Química, Facultad de Ingeniería, Universidad Nacional del Centro de la Provincia de Buenos Aires, 7400 Olavarría, Argentina
[b] Departamento de Física and Instituto IFLP (CONICET), Facultad de Ciencias Exactas, Universidad Nacional de La Plata, 1900 La Plata, Argentina
[c] Centro de Química Inorgánica (CEQUINOR/CONICET, UNLP), Facultad de Ciencias Exactas, Universidad Nacional de La Plata, C. Correo 962, 1900 La Plata, Argentina

ARTICLE INFO

Article history:
Received 30 June 2010
Received in revised form 9 August 2010
Accepted 13 August 2010
Available online 24 August 2010

Keywords:
Mixed oxides
$PbSb_2O_6$ superstructure
X-ray diffraction
Vibrational spectra
^{57}Fe-Mössbauer spectra

ABSTRACT

Four mixed oxides of composition $LnFeTeO_6$ (with Ln = La, Pr, Nd, Sm), belonging to a superstructure of the $PbSb_2O_6$ structural type, have been prepared by solid state reactions and their unit cell parameters determined by X-ray powder diffractometry. The infrared and Raman spectra of these materials were also recorded and briefly discussed, on the basis of a site-symmetry analysis. The ^{57}Fe-Mössbauer spectra show that the $Fe^{III}O_6$ octahedra present in these materials are not greatly distorted.

1. Introduction

Forty years ago Blasse and De Pauw prepared a number of mixed oxide materials belonging to the $PbSb_2O_6$ structural type, including some tellurates of the type $LaMTeO_6$ (M = Al, Ga, Fe, Rh) and $BiMTeO_6$ (M = Cr, Ga) [1]. As the number of lanthanide tellurates in general [2] and those of the type $LnMTeO_6$ in particular, remains relatively scarce we have attempted to extend the $LaFeTeO_6$ series to other Ln(III) cations, as the similar series with Cr(III), $LnCrTeO_6$, is known for all the lanthanides between La(III) and Yb(III), including Y(III) [3].

In this paper we report the synthesis of the $LnFeTeO_6$ materials with Ln = La–Sm, as well as their crystallographic data, obtained from X-ray powder measurements, complemented with the analysis of the respective vibrational (IR and Raman) and ^{57}Fe-Mössbauer spectra.

2. Experimental

2.1. Preparation of the compounds

The materials were prepared by heating, in air, well-ground stoichiomeric mixtures of Ln_2O_3, Fe_2O_3 and TeO_2 at 1000 °C during about 2 h, using platinum crucibles. The reaction mixtures were removed from the furnace intermittently, ground and reheated in order to ensure reaction completion and phase purity. The colors of the synthesized powders vary from light-brown to dark-brown, with a reddish hue in some cases. These differences in coloration are probably originated in small differences of the employed thermal treatments.

2.2. X-ray powder diagrams

The obtained mixed oxides were characterized by X-ray powder diffractometry, using a continuous step scanning procedure (step size: 0.020° (in 2θ); time per step: 0.5 s), with a Philips PW 3710 diffractometer and monochromatic Cu Kα radiation (λ = 1.54060 Å), using NaCl as an external calibration standard. The indexation of the powder diagrams and calculation of unit cell parameters were carried out using a locally modified version of the program PIRUM of Werner [4].

2.3. FTIR and Raman spectra

The infrared spectra were recorded with a Nicolet-Magna 550 FTIR instrument, using the KBr pellet technique. Raman spectra were obtained with the FRA 106 Raman accessory of a Bruker IFS 66 FTIR instrument, using the 1046 nm line of a solid state Nd:YAG laser for excitation. Spectral resolution for both measurements was ±4 cm^{-1}.

2.4. Mössbauer spectra

Room temperature Mössbauer spectra were taken in transmission geometry using a conventional constant acceleration spectrometer of 512 channels with a 10 mCi nominal activity $^{57}Co\underline{Rh}$ source, in transmission geometry. The absorber was a powdered sample, which optimum thickness was calculated with the method of Long et al. [5]. The hyperfine parameters were obtained by fitting the data to lines of Lorentzian shape using a least-squares computer code with constraints. Isomer shifts were calibrated against an α-Fe foil at room temperature.

---

* Corresponding author. Tel.: +54 221 4259485; fax: +54 221 4259485.
E-mail address: baran@quimica.unlp.edu.ar (E.J. Baran).

0925-8388/$ – see front matter © 2010 Elsevier B.V. All rights reserved.
doi:10.1016/j.jallcom.2010.08.054

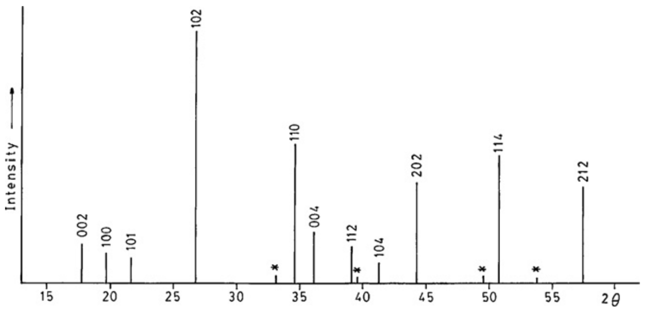

Fig. 1. Schematic representation of the indexed powder diagram of $SmFeTeO_6$. The four strongest reflections of Fe_2O_3, present as an impurity, could also be identified and are marked as (*).

3. Results and discussion

3.1. Synthesis of the compounds

As previously stated [1] the preparation of pure $LnFeTeO_6$ samples with Ln(III) other than La(III), is relatively difficult. In our preparations, we have always found small quantities of Fe_2O_3 as a contaminant. Notwithstanding, the characteristic powder pattern of $LaFeTeO_6$ [6] was found in all the prepared samples, with Ln = La–Sm, and could be successfully indexed in the hexagonal crystal system without problems. Powder diagrams of materials prepared with the smaller lanthanide cations (Gd–Lu and Y), although basically resembling the $LaFeTeO_6$ pattern, could not be indexed in this crystal system.

As an example of the obtained powder diagrams, Fig. 1 shows that corresponding to one of the prepared $SmFeTeO_6$ samples, including the calculated Miller indices and the observed reflections of Fe_2O_3, present as an impurity.

3.2. Crystallographic data and structural aspects

The $PbSb_2O_6$ structure is one of the typical structural types for AB_2O_6 mixed oxides. Its structural characteristics were first determined by Magnéli [7] and further refined by neutron powder diffraction [8]. It crystallizes in the space group $P\bar{3}1m$ and $Z = 1$, in which both Sb(V) and Pb(II) are octahedrally coordinated. Each of the SbO_6 octahedra shares three of its edges with neighboring octahedra to form an open {0 0 1} honeycomb-sheet with holes. The PbO_6-octahedra are located above and below these holes and connect adjacent SbO_6-based sheets along {0 0 1} [8–10]. Because of the large positive valence of the Sb(V) cation, the Sb–O bonding in the SbO_6 units is fairly covalent, whereas Pb–O interactions are essentially ionic [10].

Regarding the $LnCrTeO_6$ materials, it has been proposed that they may be described as a superstructure of $PbSb_2O_6$, by doubling of the *c*-parameter of the $PbSb_2O_6$ unit cell and with a long-range ordering of the Te(VI) and Cr(III) cations in the Sb(V) sublattice [1,3]. The space group of this superstructure is $P\bar{3}$ (Nr.147) with $Z = 2$ [3,11]. The same conclusions are valid for the now investigated $LnFeTeO_6$ series as its members are isostructural with the $LnCrTeO_6$ materials [1,6].

The calculated and refined unit cell parameters for the prepared $LnFeTeO_6$ compounds are shown in Table 1. A decrease of the unit cell volumes from $LaFeTeO_6$ to $SmFeTeO_6$ is clearly observable. Since the structure is built up by stacking LnO_6 and FeO_6/TeO_6 units, alternately along the *c*-axis, the volume decreases almost linearly with the diminution of the ionic radii of the big interlaying Ln(III) cations, as found also in other related compounds belonging to the $PbSb_2O_6$ structure [12]. Besides, and also due to this stacking mode of the LnO_6-polyhedra, the *c*-parameters of the unit cell show a stronger dependence from the lanthanide size, than does the corresponding *a*-parameters.

Table 1
Unit cell parameters of the investigated materials.

Material	*a* (Å)	*c* (Å)	V (Å^3)
$LaFeTeO_6$	5.203(6)	10.360(7)	242.87(3)
$PrFeTeO_6$	5.188(7)	10.147(9)	236.51(3)
$NdFeTeO_6$	5.170(4)	10.077(9)	233.25(2)
$SmFeTeO_6$	5.179(2)	9.969(4)	231.56(1)

Table 2
Site-symmetry analysis of the TeO_6 vibrational modes in the investigated $LnFeTeO_6$ materials.

"Free" TeO_6 (O_h)	Site symmetry (C_3)
ν_1 (A_{1g})	*A*
ν_2 (E_g)	*E*
ν_3 (F_{1u})	*A* + *E*
ν_4 (F_{1u})	*A* + *E*
ν_5 (F_{2g})	*A* + *E*
ν_6 (F_{2u})	*A* + *E*
Activity:	*Activity*:
A_{1g}, E_g, F_{2g}: Raman	*A*, *E*: Raman and IR
F_{1u}: IR	
F_{2u}: inactive	

3.3. Vibrational spectra

These materials show band reach IR spectral patterns in the spectral range between 700 and 300 cm^{-1}. The corresponding Raman spectra appear poorly defined, and only in the cases of $LaFeTeO_6$ and $NdFeTeO_6$ relatively well-defined spectra could be obtained.

It is expected, that these spectra are essentially dominated by vibrations related to the coordination polyhedra containing the highest charged cation, in this case the TeO_6 units, which present also relatively important covalent characteristics, as pointed out above. Therefore, and in order to analyze the vibrations of these groups, we have performed a site-symmetry analysis [13–15] on the basis of the discussed structural peculiarities, correlating the symmetry of the "free" polyhedron (O_h) with its site symmetry (C_3). The results of this analysis are presented in Table 2, and as it can be seen in the crystalline compound the degeneracy of the triple degenerated modes are partially removed and, in the crystal lattice, all vibrational modes (A and E) are IR and Raman active.

As an example of the IR spectra recorded for these materials, Fig. 2 shows that belonging to $NdFeTeO_6$. The proposed

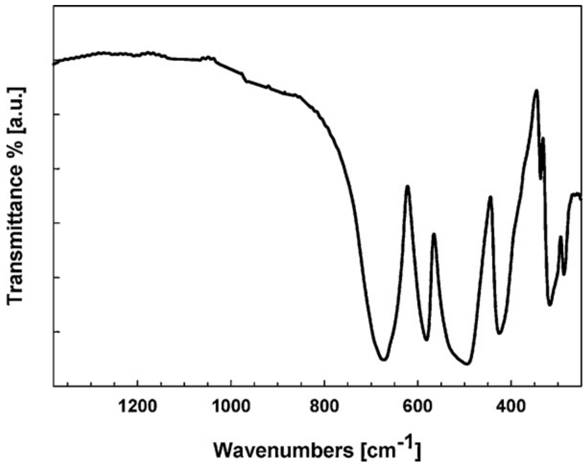

Fig. 2. FTIR spectrum of $NdFeTeO_6$.

assignment, complemented with the information provided by the corresponding Raman spectrum, is presented in Table 3, and briefly commented as follows:

- As expected, the totally symmetric stretching mode, ν_1, is seen as the strongest line in the Raman spectrum [14,16]. This vibration is not seen in the IR spectrum, because it is surely overlapped with the very strong and broad ν_3 band.
- The predicted splitting of the triple degenerated modes (cf. again Table 2) is not clearly visualized neither in the IR nor in the Raman spectrum. Notwithstanding, the IR band assigned to the ν_4 vibration is clearly asymmetric, presenting a weak shoulder on its higher energy side. Besides, the Raman band assigned to ν_3 presents also a weak splitting on the high energy edge.
- The relatively high energy and IR-intensity of the ν_2 mode is especially remarkable, whereas in the Raman spectrum the line related to this vibration shows only a very weak intensity.
- Bands assignable to the predicted components of the ν_6 vibrational mode could not be identified, probably because this vibration attains not enough intensity. The position of this band is expected to lie at about 300 cm^{-1}, as predicted by the known relation $\nu_6 = \nu_5\sqrt{2}$ [17].
- The IR band doublet at 337/317 cm^{-1} and its Raman counterpart (a single weak band at 340 cm^{-1}) has been tentatively assigned to stretching vibrations of the FeO_6 and LnO_6 octahedra, by comparison with characteristic vibrations of Fe_2O_3 and lanthanide oxides [13,18,19].
- Vibrations below 300 cm^{-1} can confidently be assigned to external (lattice) modes [13,16,20].

It is also interesting to comment, that the proposed assignments agrees very well with those given for the TeO_6 vibrations in some ordered perovskite tellurates, such as Sr_2NiTeO_6, Ba_2CaTeO_6 and Ca_3TeO_6 [20].

Finally, it seems interesting to perform a rough estimation of the force constants of the analyzed Te–O bonds. On the basis of the G and F matrixes for a regular octahedral species [21], neglecting coupling between the two F_{1u} vibrations and assuming $f_{rr} = f'_{rr}$ the following simplified equations can be formulated for this purpose (cf. [22,23]):

$$\lambda_s = \mu_O(f_r + 5f_{rr}) \quad (A_{1g})$$

$$\lambda_{as} = (\mu_O + 2\mu_{Te})(f_r - f_{rr}) \quad (F_{1u})$$

Resolving these equations using the ν_1 and ν_3 values presented in Table 3, a value of 3.43 mdyn/Å is obtained for the f_r value of the Te–O bond, whereas the corresponding bond–bond interaction constant, f_{rr}, lies at 0.23 mdyn/Å. The bond order, according to Siebert [15], estimated from the calculated force constant f_r is 1.11, pointing to a weak Te–O bond with a practically negligible π-contribution.

The band positions of the measured FTIR spectra of the complete series of investigated compounds are shown in Table 4. As it can be seen, most of the IR bands show a weak but clear displacement to higher wavenumbers which parallels the diminution of the unit cell volumes. This is the usually expected trend for a series of isostructural compounds of this type, and is related to the reinforcement of the Te–O bonds with the diminution of the unit cell dimensions [24–26].

Table 3
Assignment of the IR and Raman spectra of $NdFeTeO_6$ (band positions in cm^{-1}).

Infrared	Raman	Approximate assignment
	715 vs	ν_1 (TeO_6), symmetric Te–O stretching
675 vs, br	670 m	ν_3 (TeO_6), antisymmetric Te–O stretching
582 vs	610 vw	ν_2 (TeO_6), symmetric Te–O stretching
530 sh, 495 vs, br	490 s	ν_4 (TeO_6), antisymmetric deformation
426 vs	433 w	ν_5 (TeO_6), antisymmetric deformation
337 m, 317 s	340 w	ν (FeO_6)/ν (LnO_6)
287 m		External mode

vs, very strong; s, strong; m, medium; w, weak; br, broad; sh, shoulder.

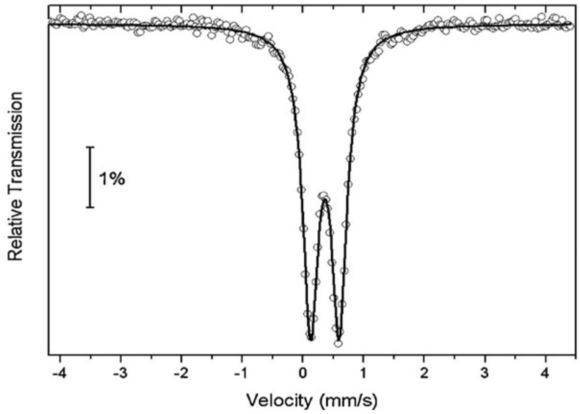

Fig. 3. ^{57}Fe-Mössbauer spectrum of $NdFeTeO_6$.

Table 5
Mössbauer parameters of the investigated compounds.

Compound	δ (mm/s)	Δ (mm/s)	Γ (mm/s)
$LaFeTeO_6$	0.36 ± 0.01	0.45 ± 0.02	0.26 ± 0.01
$PrFeTeO_6$	0.35 ± 0.01	0.46 ± 0.02	0.26 ± 0.01
$NdFeTeO_6$	0.35 ± 0.01	0.47 ± 0.01	0.30 ± 0.01
$SmFeTeO_6$	0.34 ± 0.01	0.49 ± 0.02	0.32 ± 0.02

3.4. *Mössbauer spectra*

Fig. 3 shows the ^{57}Fe-Mössbauer spectrum of $NdFeTeO_6$, as a typical example of the obtained spectra. The determined hyperfine parameters (chemical shift, δ; quadrupolar splitting, Δ; line half-width, Γ) are presented in Table 5.

The measured isomeric shifts falls clearly in the range which is characteristic for high-spin Fe(III) in an octahedral oxygen environment [27,28]. On the other hand, the values of the quadrupolar

Table 4
Assignment of the IR spectra of the investigated $LnFeTeO_6$ materials (band positions in cm^{-1}).

$LaFeTeO_6$	$PrFeTeO_6$	$NdFeTeO_6$	$SmFeTeO_6$	Approximate assignment
670 vs, br	671 vs	675 vs, br	673 vs, br	ν_3 (TeO_6)
577 s	578 s	582 vs	584 s	ν_2 (TeO_6)
520 sh, 495 vs	535 sh, 495 vs	530 sh, 495 vs	525 sh, 501 vs	ν_4 (TeO_6)
420 s	420 s	426 s	428 s	ν_5 (TeO_6)
334 m, 311 s	335 m, 314 s	337 m, 317 s	340 m, 320 s	ν (FeO_6)/ν (LnO_6)
281 s	282 s	287 m	289 m	External modes

vs, very strong; s, strong; m, medium; br, broad; sh, shoulder.

splittings show that the FeO_6-polyhedra are not very distorted. Interestingly, these values show a certain tendency to increase on going from $LaFeTeO_6$ to $SmFeTeO_6$, suggesting a slightly increasing distortion with the diminution of the unit cell volumes, as observed in other cases [26].

4. Conclusions

Four mixed tellurate oxides of composition $LnFeTeO_6$ (with Ln = La, Pr, Nd, Sm) were prepared by solid state reaction. They are isostructural with the corresponding $LnCrTeO_6$ materials, belonging to a superstructure of the $PbSb_2O_6$ structural type. Their unit cell parameters were determined by X-ray powder diffractometry. The FTIR and FT-Raman spectra of these materials were also recorded and briefly discussed on the basis of a site-symmetry analysis, derived from the structural characteristics. A rough estimation of the force constants for the Te–O bonds of the TeO_6-polyhedra was also performed, showing the presence of relatively weak bonding. The ^{57}Fe-Mössbauer spectra show chemical shifts which are characteristic for high-spin Fe(III) in octahedral oxide coordination and also show that the $Fe^{III}O_6$-polyhedra present in these materials are scarcely distorted.

Acknowledgements

This work has been supported by the Universidad Nacional de La Plata, the Universidad Nacional del Centro de la Provincia de Buenos Aires and the Consejo Nacional de Investigaciones Científicas y Técnicas de la República Argentina. R.C.M. and E.J.B. are members of the Research Career from this organization.

References

[1] G. Blasse, A.D.M. De Pauw, J. Inorg. Nucl. Chem. 32 (1970) 2533.
[2] J. Llanos, R. Castillo, D. Barrionuevo, D. Espinoza, S. Conejeros, J. Alloys Compd. 485 (2009) 565.
[3] H.M. Kasper, Mater. Res. Bull. 4 (1969) 33.
[4] P.E. Werner, Ark. Kemi 31 (1969) 51.
[5] J. Long, T.E. Cranshaw, G.M. Longworth, Mössbauer Effect Refer. Data J. 6 (1983) 42.
[6] N.K. Gupta, S.P. Roy, P.V. Joshi, G.A. Rama Rao, K. Krishnan, K.D. Singh Mudher, J. Alloys Compd. 417 (2006) 300.
[7] A. Magnéli, Ark. Kemi Min. Geol. 15B (3) (1941).
[8] R.J. Roderick, J. Solid State Chem. 71 (1987) 12.
[9] M. Weil, T. Dordević, C.L. Lengauer, U. Kolitsch, Solid State Sci. 11 (2009) 2111.
[10] H. Mizoguchi, P.M. Woodward, Chem. Mater. 16 (2004) 5233.
[11] Inorganic Crystal Structure Database (ICSD), ICSD#164936, FIZ-Karlsruhe, Karlsruhe, Germany.
[12] N. Kumada, T. Takei, N. Kinomura, H. Wang, X.X. Zhang, H. Yan, Mater. Res. Bull. 40 (2005) 1166.
[13] S.D. Ross, Inorganic Infrared and Raman Spectra, McGraw-Hill, London, 1972.
[14] A. Müller, E.J. Baran, R.O. Carter, Struct. Bond. 26 (1976) 81.
[15] A. Fadini, F.M. Schnepel, Vibrational Spectroscopy. Methods and Applications, Ellis Horwood Ltd., Chichester, 1989.
[16] A.F. Corsmit, H.E. Hoefdraad, G. Blasse, J. Inorg. Nucl. Chem. 34 (1972) 3401.
[17] A. Fadini, I. Joss, S. Kemmler-Sack, G. Rauser, H.J. Rother, E. Schillinger, H.J. Schittenhelm, U. Trieber, Z. Anorg. Allg. Chem. 439 (1978) 35.
[18] N.T. McDevitt, W.L. Baun, Spectrochim. Acta 20 (1964) 799.
[19] N.T. McDevitt, A.D. Davidson, J. Opt. Soc. Am. 56 (1966) 638.
[20] G. Blasse, A.F. Corsmit, J. Solid State Chem. 6 (1973) 513.
[21] J.R. Ferraro, J.S. Ziomek, Introductory Group Theory and its Applications to Molecular Structure, Plenum Press, New York, 1969.
[22] A. Müller, E.J. Baran, J. Hauck, Spectrochim. Acta 31A (1975) 801.
[23] E.J. Baran, M. Weil, Spectrochim. Acta 61A (2005) 707.
[24] A.E. Lavat, M. Trezza, I.L. Botto, D.I. Roncaglia, E.J. Baran, Spectr. Lett. 21 (1988) 355.
[25] A.E. Lavat, E.J. Baran, R. Sáez-Puche, A. Salinas-Sánchez, M.J. Martin-Llorente, Vib. Spectrosc. 3 (1992) 291.
[26] E.J. Baran, R.C. Mercader, C. Cascales, J. Phys. Chem. Solids 65 (2004) 1913.
[27] P. Gütlich, R. Link, A. Trautwein, Mössbauer Spectroscopy and Transition Metal Chemistry, Springer, Berlin, 1978.
[28] F. Menil, J. Phys. Chem. Solids 46 (1985) 763.